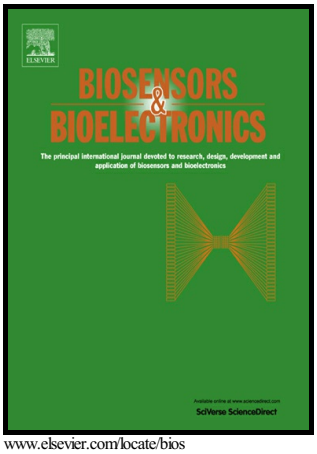

www.elsevier.com/locate/bios

Fluorescence biosensing strategy based on mercury ion-mediated DNA conformational switch and nicking enzyme-assisted cycling amplification for highly sensitive detection of carbamate pesticide

Xiuzhong Wang, Ting Hou, Shanshan Dong, Xiaojuan Liu, Feng Li

PII: S0956-5663(15)30498-X
DOI: http://dx.doi.org/10.1016/j.bios.2015.10.034
Reference: BIOS8070

To appear in: *Biosensors and Bioelectronic*

Received date: 3 August 2015
Revised date: 29 September 2015
Accepted date: 11 October 2015

Cite this article as: Xiuzhong Wang, Ting Hou, Shanshan Dong, Xiaojuan Liu and Feng Li, Fluorescence biosensing strategy based on mercury ion-mediated DNA conformational switch and nicking enzyme-assisted cycling amplification for highly sensitive detection of carbamate pesticide, *Biosensors and Bioelectronic,* http://dx.doi.org/10.1016/j.bios.2015.10.034

Fluorescence biosensing strategy based on mercury ion-mediated DNA conformational switch and nicking enzyme-assisted cycling amplification for highly sensitive detection of carbamate pesticide

Xiuzhong Wang, Ting Hou, Shanshan Dong, Xiaojuan Liu, Feng Li*

College of Chemistry and Pharmaceutical Sciences, Qingdao Agricultural University, Qingdao 266109, P.R. China

Submitted to ***Biosensors & Bioelectronics,*** Aug. 3, 2015; Revised Sep. 29, 2015

* Corresponding author. E-mail: lifeng@qust.edu.cn; Tel/Fax: +86-532-86080855

Abstract

Pesticides are of great importance in agricultural and biological fields, but pesticide residues may harm the environment and human health. A highly sensitive fluorescent biosensor for the detection of carbamate pesticide has been developed based on acetylcholinesterase (AChE)-catalyzed hydrolysis product triggered

Hg^{2+} release coupled with subsequent nicking enzyme-induced cleavage of a duplex DNA for cycling amplification. In this protocol, two DNA probes, an unmodified single-stranded helper DNA probe 1 (HP1) and a quencher–fluorophore probe (QFP) are ingeniously designed. HP1 can be folded into hairpin configuration through T–Hg^{2+}–T base pair formation. QFP, labeled with FAM and BHQ1 at its two terminals, contains the recognition sequence and the cleavage site of the nicking enzyme. In the presence of carbamate pesticide, the activity of AChE is inhibited, and the amount of the product containing the thiol group generated by the hydrolysis reaction of acetylcholine chloride (ACh) decreases, resulting in the release of a low concentration of Hg^{2+}. The number of HP1 that can be selectively unfolded would be reduced and the subsequent nicking enzyme-assisted cleavage processes would be affected, resulting in decreased fluorescence signals. The fluorescence intensity further decreases with the increase of the pesticide concentration. Therefore, the pesticide content can be easily obtained by monitoring the fluorescence signal change, which is inversely proportional to the logarithm of the pesticide concentration. The detection limit of aldicarb, the model analyte, is 3.3 μg L^{-1}, which is much lower than the Chinese National Standards or those previously reported. The as-proposed method has also been applied to detect carbamate pesticide residues in fresh ginger and artificial lake water samples with satisfactory results, which demonstrates that the method has great potential for practical application in biological or food safety field.

Keywords: DNA probe; Nicking enzyme; Signal amplification; Fluorescent detection; Carbamate pesticide

1. Introduction

Pesticides, including diverse classes of carbamates, organophosphates, organochlorine, pyrethroids and so on, are used to protect plants and crops from insects and pests infestations in agriculture across the world (Aragay et al. 2012; Llorent Martinez et al. 2011). Carbamates and organophosphates are the most widely used insecticides and pesticides, due to the relatively low persistence under natural conditions and high effectiveness for insect and pest eradication (Qian and Lin 2015). Carbamate pesticides, esters derived from carbamic acid, are one of the major classes of highly effective commercial pesticides which are used more widely than organophosphorous and organochlorine pesticides in recently years (Zhang et al. 2013a). However, carbamates are considered to be hazardous to the environment and human health (Miao et al. 2010), and they are on the priority list released by the U.S. Environmental Protection Agency (EPA). Carbamate pesticides are only allowed to be used in food crops and stored grain in China (Zhou et al. 2009). The high toxicity of carbamates is ascribed to their capability of irreversibly inhibiting the activity of acetylcholinesterase (AChE) in the central and peripheral nervous system, resulting in accumulation of the neurotransmitter acetylcholine (ACh) in the body, thus leading to fatal consequences (Feng et al. 2007; Li et al. 2014; Liu et al. 2012; Pardo Yissar et al. 2003). Therefore, the detection of carbamates is very important for both human health and environmental protection.

In the past decade, many efforts have been made to develop efficient methods to assay carbamates in agricultural products, waters and soils. For examples, gas chromatography/mass spectrometry (Lee and Lee 2011; Zhou et al. 2012), high-performance liquid chromatography (Nanita et al. 2009; Wang et al. 2014a), electrochemical analysis (Oliveira et al. 2013; Rao et al. 2002; Upadhyay et al. 2009; Zhang et al. 2011), and spectroanalysis methods (Azab et al. 2012; Liu et al. 2012; Qian and Lin 2015) have been developed for analyzing carbamate pesticides. Although these methods show high selectivity, adequate sensitivity and

allow discrimination of pesticides, solvent extraction procedures are generally involved, which are time-consuming, expensive, and rely on sophisticated instruments and skilled manpower, making these approaches impractical for routine environment and food safety monitoring. Rapid methods for sensitive and selective detection of carbamate pesticide residues are therefore highly desirable. Biosensors present a promising alternative to conventional techniques as they offer a rapid, specific, and sensitive way for the detection of environmental pollutants, including pesticides, without the need of sophisticated instruments (Kim et al. 2007; Suwansa ard et al. 2005; Yao et al. 2013). Among these biosensing methods, AChE-based biosensors have been widely explored for the detection of several classes of pesticides (Schulze et al. 2003; Yi et al. 2013; Chauhan and Pundir 2014; Lu and Xia 2015). For example, Zamfir et al. proposed a biosensor based on AChE-inhibition effects for the detection of two carbamate therapeutic drugs, with the AChE immobilized in sol–gel matrix (Zamfir et al. 2013). According to previous reports, in most cases the AChE was immobilized onto the complicated matrix and even sometimes modification or functionalization of AChE is inevitable in order to improve the detective sensitivity (Kim et al. 2007). The complicated and tedious modification processes could negatively impact the structure and the function of the enzyme (such as lowering the AChE activity) (Liu et al. 2011; Periasamy et al. 2009). Moreover, the recognition efficiency of the substrate in the multiphase structure is usually lower than that in the homogeneous solution because of the interface steric hindrance effect. Hence, it is urgent to develop new sensing strategies which are highly sensitive and accurate, yet still avoid the immobilization of the enzyme to ensure activity and catalytic efficiency in the AChE-based pesticide assay systems.

Owing to the high stability, remarkable molecular recognition property and easy modification, deoxyribonucleic acid (DNA) probes have been immensely employed to build smart devices for applications in biomedicine, sensing and material science. For example, Zhang et al. proposed a signal-on

fluorescent biosensor based on DNA-templated silver nanoclusters for rapid, ultrasensitive assay of AChE (Zhang et al. 2013b). In order to improve the assay sensitivity, many efforts have been focused on the design that utilizes enzymes as signal amplifying elements (Cheglakov et al. 2006; Cheglakov et al. 2007; Huang et al. 2013; Tang et al. 2012). Among these nucleic acid amplification-based techniques, nicking enzyme amplification reaction (NEAR), which provides a simple and general strategy for signal amplification, is a method for in vitro DNA amplification like the polymerase chain reaction (PCR), but as compared to PCR, NEAR has the advantages of increased speed, reduced cost, lower energy requirements and the ability to be carried out in field (Song et al. 2014).

DNA–metal base pairs currently attract considerable attention because of their potential in sensing applications (Li et al. 2009). Some metal ions can selectively bind to a few native or artificial bases in DNA duplexes to form metal-mediated base pairs (Zhu et al. 2014). Hg^{2+} is found to specifically interact with the thymine–thymine (T–T) mismatch in DNA duplexes (Ma et al. 2015; Miyake et al. 2006). This generally increases the thermal stability of DNA duplexes. For instance, He et al. reported a smart strategy for label-free sensitive DNA detection using the dopant Hg^{2+} ions which were initially sequestered in the hairpin structured probe through T–Hg^{2+}–T mismatch formation (He and Ma 2014).

Inspired by the above-mentioned works, herein, we construct a highly sensitive fluorescent biosensor for the detection of carbamate pesticide based on AChE hydrolysis product-triggered Hg^{2+} release coupled with subsequent nicking enzyme-induced cleavage of a duplex DNA for cycling signal amplification. To the best of our knowledge, no such method has yet been reported. For the proof-of-concept experiment, aldicarb, an extremely toxic carbamate insecticide often used on crops, was employed as a model analyte to examine the desirable properties of this assay. This simple and sensitive method has been developed to determine carbamate pesticide based on its inhibition on AChE activity, and has also been applied to detect

pesticide residue in fresh ginger and artificial lake water samples. Therefore, it is believed that this strategy possesses great potential to be applied in the field of food safety for simple, sensitive and convenient detection of carbamate pesticide residues in all sorts of samples.

2. Experimental

2.1. Reagents and materials

The HPLC-purified oligonucleotides were purchased from Sangon Biotech. Co., Ltd. (Shanghai, China), and their sequences are listed in Table 1. Acetylcholinesterase (AChE, 220 U g^{-1}, from *Electrophorus electricus*) and acetylthiocholine chloride (ACh) were purchased from Sigma-Aldrich (St. Louis, MO, USA) and used as supplied. Aldicarb was purchased from Aladdin (Shanghai, China). Nb.BtsI (10000 U mL^{-1}) and 1 × NEBuffer 4 solution were purchased from New England Biolabs (Ipswich, MA, USA). $Hg(NO_3)_2$ was purchased from Shenzhen Bolinda Technology (Shenzhen, China). Cleanert PSA、C18 and GCB were purchased from Agela Technologies Inc. (Tianjin, China). Ultrapure water (18.2 MΩ cm at 25℃) obtained from a Milli-Q water purification system (Millipore Corp., Bedford, MA) was used throughout the experiments. All chemicals are of analytical grade and used without further purification.

<<Herein Table 1>>

2.2. Apparatus

All fluorescence measurements were performed on a Hitachi F-4600 fluorescence spectrometer (Japan) equipped with a xenon lamp as the excitation source and a personal computer as the data processing unit. The slits for excitation and emission were both set at 5.0 nm and the photomultiplier tube voltage was 700 V. The excitation wavelength was set at 497 nm, and the emission spectra from 505 to 650 nm were collected. The fluorescence intensity at 525 nm was used to evaluate the performance of the proposed strategy. All fluorescence detections were carried out at room temperature unless otherwise indicated.

2.3. Fluorescence assay for aldicarb

All oligonucleotides were used as provided and diluted in 1 × NEBuffer 4 solution (50 mM potassium acetate, 20 mM tris-acetate, 10 mM magnesium acetate, pH 7.9) to give the stock solutions. To carry out the assay, firstly, HP1 and Hg^{2+} ions were mixed with a molar ratio of 1:3 to generate three T–Hg^{2+}–T base pairs in each probe molecule (He and Ma 2014). Secondly, aldicarb with different concentrations and 1 mU mL^{-1} AChE were incubated in a 1 × NEBuffer 4 solution (pH 6.8) for 30 min at 37 °C. Thirdly, 0.03 μM ACh, 5 nM HP1, 250 nM QFP and 100 U mL^{-1} Nb.BtsI enzyme were incubated for 120 min in 1 × NEBuffer 4 solution (pH 7.9) for fluorescence assay. The same processing procedure without aldicarb was used as the control experiment.

3. Results and discussion

3.1. Principle of fluorescence assay for pesticide

The principle of the proposed fluorescence assay for pesticide is illustrated in Fig. 1, in which aldicarb is adopted as the model analyte. The system mainly consists of HP1, QFP, ACh, AChE and Nb.BtsI enzyme. HP1, an unmodified single-stranded oligonucleotide is ingeniously designed, which can form hairpin structure through T–Hg^{2+}–T base pair formation by incorporating Hg^{2+} ions into the stem. Formation of T–Hg^{2+}–T base pair is highly efficient and specific to T–T mismatch and Hg^{2+} ion (Miyake et al. 2006; Shi et al. 2014; Zhu et al. 2014). QFP, in which the fluorescence of the fluorophore (FAM) at one end is quenched by the quencher (BHQ1) at the other end due to the fluorescence resonance energy transfer (FRET) effect (Wang et al. 2014b), can not only fully hybridize with part of HP1 to form duplex DNA once the hairpin structure is unfolded, but also contain the recognition sequence as well as the cleavage site for Nb.BtsI.

<<Herein Fig. 1>>

In the absence of aldicarb, AChE catalyzes the hydrolysis reaction of ACh to generate thiocholine, which contains the chemically reactive thiol group (–SH) and plays an essential role in this protocol (Zhao et al. 2013). Due to the stronger S–Hg interaction, upon the reaction with thiocholine, Hg^{2+} ions would be released from the hairpin structure of HP1. As a result, the configuration of HP1 changes from the hairpin to the single-stranded structure, because the binding force between the residual three G – C and one A – T complementary base pairs in the stem of the probe is not sufficient enough to maintain the stable hairpin structure (Xing et al. 2014). Subsequently, the linear strand of HP1 in turn can easily hybridize with QFP to form complementary double-stranded structure. Once the DNA duplex is formed, the nicking enzyme Nb.BtsI recognizes and cleaves QFP. So the fluorophore in QFP is separated from the quencher to restore its fluorescence signal, and at the same time HP1 is released to hybridize with other un-cleaved QFP repeatedly, initiating the cycle of nicking–dissociation–hybridization for significant fluorescence enhancement.

In contrast, in the presence of the pesticide aldicarb, the activity of AChE is inhibited. The amount of the product containing the thiol group generated by the hydrolysis reaction of ACh is thus reduced, resulting in the release of less Hg^{2+} originally embedded in the stem of HP1. The number of the hairpin structure of the HP1 that can be selectively opened is then reduced and the subsequent nicking enzyme-assisted cleavage processes is retarded, resulting in decreased fluorescence signals. Moreover, the fluorescence intensity further decreases with the increase of aldicarb concentration. Therefore, by this “signal-off” mode, the pesticide content could be easily detected by monitoring the fluorescence signal change.

3.2. Feasibility study of aldicarb detection

To illustrate the feasibility of this strategy, the proof-of-concept experiments were carried out for aldicarb detection. The fluorescence intensities of the system under different conditions were measured and

the corresponding fluorescence spectra are shown in Fig. 2.

<<Herein Fig. 2>>

In the presence of QFP only, the fluorescence intensity was relatively weak (carve a), demonstrating that the fluorescence of the fluorophore (FAM) at one end was quenched by the quencher (BHQ1) at the other end due to the FRET effect. In the presence of HP1 (with a hairpin configuration) and QFP, the fluorescence spectrum (curve b) was almost the same as that of QFP (carve a). After Nb.BtsI enzyme was added into the solution containing HP1 and QFP, the fluorescence intensity of the system exhibited a slight enhancement (curve c). The fluorescence spectrum (curve d) was almost the same as curve c in the presence of ACh without AChE. However, in the presence of ACh, AChE, HP1, QFP and Nb.BtsI enzyme, significant fluorescence enhancement was observed (curve e), indicating that AChE catalyzed the hydrolysis reaction of ACh to generate the product containing the chemically reactive thiol groups. Then the thiol groups competitively bound with Hg^{2+} embedded in the stem of HP1, unfolding the hairpin configuration. Once the linear HP1 strand was formed, the subsequent autonomous Nb.BtsI enzyme-assisted cleavage cycle processes were initiated. In the presence of carbamate pesticide aldicarb, the activity of AChE was inhibited (or partially inhibited) and thus the generation of the hydrolysis product containing the thiol group was inhibited, accompanied by the decrease of the fluorescence intensity (curve f). The aforementioned results clearly demonstrated the feasibility of the proposed fluorescence biosensing platform for carbamate pesticide detection.

Recently, the possible inhibiting effect of Hg^{2+} on Exo III activity was reported (Yuan et al. 2012), so the inhibiting effect of Hg^{2+} on Nb.BtsI activity was tested. To simplify the operation steps, another single-stranded helper DNA probe HP2, which is perfectly complementary with QFP, substitute for HP1 to execute the assay. As shown in Fig. S1, the high fluorescence intensities remained almost constant with the

concentration of Hg^{2+} increased from 0 to 25 nM, indicating that Nb.BtsI can effectively cleave duplex DNA and the activity of Nb.BtsI is not affected by Hg^{2+}. Besides, the effect of aldicarb on Nb.BtsI activity was also tested. As shown in Fig. S2, the fluorescence intensities decreased slightly in the presence of aldicarb with high concentration. However, the decrease of the fluorescence intensity is negligible because of very low concentration of pesticide present in real samples.

3.3. Optimization of experimental conditions

The sensing mechanism of this protocol is based on the irreversible inhibition capability of carbamate pesticide on the activity of AChE, which leads to the reduction of fluorescence intensity. So all experimental conditions have been optimized to ensure the highest fluorescence signal in the absence of pesticide.

The enzyme activity is strongly concentration and pH-dependent, so the concentration of AChE and pH for the hydrolysis reaction of ACh were firstly investigated. Fig. 3A shows the effect of the concentration of AChE on the fluorescence intensity of the system. It is observed that fluorescence intensities obviously enhanced with the increase of AChE concentration. The highest fluorescence intensity was acquired at the AChE concentration of 1.0 mU mL^{-1}. However, a noticeable decrease of the fluorescence intensity was observed when the concentration exceeded 1.0 mU mL^{-1}. As shown in Fig. 3B, the fluorescence intensity increased with the increase of the pH value and kept stable between pH 6.8 and 7.6. However, the fluorescence intensity decreased with the further increase of the pH value. However, carbamate pesticides were easily oxidized in basic solutions, so the pH of the buffer solution was preferred to be lower than 7.0 (Lin and Chen 2006). According to the above results, therefore, 1.0 mU mL^{-1} AChE and pH 6.8 were employed for the following experiments.

<< Herein Fig. 3 >>

Other experimental conditions, such as the reaction temperature, the enzymatic reaction time for the hydrolysis of ACh by AChE and the Nb.BtsI enzyme-triggered cycling amplification reaction can also affect the detection sensitivity. A series of conditional experiments were carried out to improve the assay sensitivity. Lower temperature may be beneficial to the stability of Hg^{2+}-induced hairpin structure but is disadvantageous to the activity of AChE for the hydrolysis reaction of ACh. As can be seen from Fig. 4A, the fluorescence intensity of the system initially increased with the temperature increased from 25 to 37 °C owing to the enhancement of the enzyme activity, but the fluorescence intensity decreased gradually when the temperature was further increased to 55 °C, which may arise from the partial loss of AChE activity or the dissociation of certain amount of duplex DNA formed between QFP and HP1. The fluorescence intensity increased along with the increase of the hydrolysis reaction time of ACh and leveled off at 30 min (Fig. 4B), and similarly the fluorescence intensity reached the maximum value at 120 min for the Nb.BtsI enzyme-triggered cycling amplification reaction (Fig. S3). After comprehensive consideration, the optimal reaction temperature, reaction times for the hydrolysis of ACh and the Nb.BtsI enzyme-triggered cycling amplification were chosen to be 37 °C, 30 min and 120 min, respectively.

<<Herein Fig. 4>>

3.4. Analytical performance of the fluorescence pesticide assay

To demonstrate the applicability of the designed strategy for quantitative fluorescence detection of carbamate pesticides, aldicarb was selected as the model analyte. Under the optimal experimental conditions, it was evaluated by monitoring the fluorescence change under different concentrations of aldicarb. As shown in Fig. 5, by increasing the concentration of aldicarb, the fluorescence intensity decreased gradually. As shown in the inset of Fig. 5B, the fluorescence intensity showed a good linear relationship with the logarithm of the aldicarb concentration ranging from 10 to 10000 μg L^{-1}. The linear regression equation was $F = -144.5\ Log_{10}\ c + 653.6$ with the correlation coefficient of 0.996 (F: fluorescence intensity, c: aldicarb concentration (μg L^{-1})). The detection limit was estimated to be 3.3 μg

L^{-1} (based on signal-to-noise ratio of 3), which is lower than those of the previously reported sensors (Abad et al. 1998; Oliveira et al. 2013; Zamfir et al. 2013) and Chinese National Standards (50 μg L^{-1}). The results demonstrated that highly sensitive fluorescence detection of carbamate pesticides can be realized.

<<Herein Fig. 5>>

The selectivity of the sensing system was further investigated by substituting aldicarb with four different kinds of pesticides, namely chlordane, dimethoate, pyrethroids and endosulfan, respectively. As shown in Fig. S4, decreasing fluorescence signal was obtained only in the presence of the aldicarb. The fluorescence intensities were barely changed in the presence of chlordane, dimethoate, pyrethroids or endosulfan, which were comparable to the background signal. These data demonstrated that the fluorescence signal was specifically triggered by the carbamate pesticides based on the inhibition of AChE activity for parallel samples, which indicated that the strategy we proposed here exhibited good performance for discriminating aldicarb from other interfering pesticides. Thus, due to the excellent selectivity, the as-proposed fluorescence assay for carbamate pesticides has great potential to be applied in samples with complex substrates.

3.5. Detection of pesticide residues in real samples

Pesticide residues in fresh ginger and artificial lake water samples were also detected by the as-proposed fluorescence strategy to investigate its applicability in real samples. Fresh ginger was obtained from local farmer market and water sample was obtained from the artificial lake in Qingdao Agricultural University, and QuEChERS extraction method (Seiber and Kleinschmidt 2011; Wang et al. 2014a) was adopted to extract aldicarb. It was found that the content of pesticides were all below the detection limit in these two samples. Furthermore, the fluorescence tests were performed by adding different amounts of aldicarb in the samples. Spiked samples with aldicarb concentrations of 100, 500 and 1000 μg L^{-1} were analyzed and six repetitive measurements were carried out for each sample. The experimental results are presented in Table S1.

Acceptable recoveries (from 92% to 104% for fresh ginger and from 96.5% to 102% for artificial lake water) were attained. These results demonstrate that the as-proposed biosensing system exhibits good anti-interference capability, even in complex matrix, and therefore has great potential in practical applications.

4. Conclusions

In summary, we have successfully developed a sensitive, convenient, low-cost fluorescence strategy for pesticide detection based on AChE-catalyzed hydrolysis triggered Hg^{2+} release-induced DNA conformational change coupled with subsequent nicking enzyme assisted signal amplification. This method relies on the significant fluorescence decrease resulting from the inhibition of the activity of the AChE by pesticides, and the fluorescence intensity decreased with the increase of the pesticide concentration. The detection limit is 3.3 μg L^{-1} for aldicarb, which is much lower than the Chinese National Standards (50 μg kg^{-1}) or those reported by previous fluorescence methods. This method also exhibits good applicability for aldicarb detection in real samples. In addition, the AChE need not be immobilized on complex substrate which can benefit for its high biologically activity. Taken together, the assay shows great potential for practical application in biological or food safety fields and will be competent for the great demand for determination of carbamate pesticides.

Acknowledgements

This work was funded by the National Natural Science Foundation of China (Nos. 21405089, 21375072, 21575074), the Scientific Research Award Fund for Excellent Middle-aged and Young Scientists of Shandong Province (Nos. BS2014CL004, BS2013DX025), the Basic Research Program of Qingdao (No.13-1-4-226-jch) and the Research Foundation for Distinguished Scholars of Qingdao Agricultural University (No. 663-1113311).

References

Abad, J.M., Pariente, F., Hernández, L., Abruña, H.D., Lorenzo, E., 1998. Anal. Chem. 70(14), 2848–2855.

Aragay, G., Pino, F., Merkoçi, A., 2012. Chem. Rev. 112, 5317–5338.

Azab, H.A., Duerkop, A., Saad, E.M., Awad, F.K., Abd El Aal, R.M., Kamel, R.M., 2012. Spectrochim Acta A 97, 915–922.

Chauhan, N., Pundir, C.S., 2014. Biosens. Bioelectron. 61, 1–8.

Cheglakov, Z., Weizmann, Y., Beissenhirtz, M.K., Willner, I., 2006. Chem. Commun.(30), 3205–3207.

Cheglakov, Z., Weizmann, Y., Basnar, B., Willner, I., 2007. Org. Biomol. Chem. 5(2), 223–225.

Feng, F.D., Tang, Y.L., Wang, S., Li, Y.L., Zhu, D.B., 2007. Angew. Chem. Int. Ed. 46, 7882–7886.

He, X.W., Ma, N., 2014. Anal. Chem. 86, 3676–3681.

Huang, Y., Chen, J., Zhao, S.L., Shi, M., Chen, Z.F., Liang, H., 2013. Anal. Chem. 85(9), 4423–4430.

Kim, N., Park, I.S., Kim, D.K., 2007. Biosens. Bioelectron. 22(8), 1593–1599.

Lee, J., Lee, H.K., 2011. Anal. Chem. 83(17), 6856–6861.

Li, H.C., Guo, Y.X., Xiao, L.H., Chen, B., 2014. Analyst 139, 285–289.

Li, T., Shi, L.L., Wang, E.K., Dong, S.J., 2009. Chem. Eur. J. 15, 3347–3350.

Lin, Z.Y., Chen, G.N., 2006. Talanta 70(1), 111–115.

Liu, D.B., Chen, W.W., Wei, J.H., Li, X.B., Wang, Z., Jiang, X.Y., 2012. Anal. Chem. 84, 4185–4191.

Liu, T., Su, H.C., Qu, X.J., Ju, P., Cui, L., Ai, S.Y., 2011. Sens. Actuators B: Chem. 160(1), 1255–1261.

Llorent Martinez, E.J., Ortega Barrales, P., Fernandez de Cordova, M.L., Ruiz Medina, A., 2011. Anal. Chim. Acta 684(1–2), 21–30.

Lu, L.L., Xia, Y.S., 2015. Anal. Chem. 87(16), 8584–8591.

Ma, Z.Y., Pan, J.B., Lu, C.Y., Zhao, W.W., Xu, J.J., Chen, H.Y., 2015. Chem. Commun. 50, 12088–12090.

Miao, Y.Q., He, N.Y., Zhu, J.J., 2010. Chem. Rev. 110, 5216–5234.

Miyake, Y., Togashi, H., Tashiro, M., Yamaguchi, H., Oda, S., Kudo, M., Tanaka, Y., Kondo, Y., Sawa, R., Fujimoto, T., Machinami, T., Ono, A., 2006. J. Am. Chem. Soc. 128(7), 2172–2173.

Nanita, S.C., Pentz, A.M., Bramble, F.Q., 2009. Anal. Chem. 81(8), 3134–3142.

Oliveira, T.M.B.F., Fátima Barroso, M., Morais, S., Araújo, M., Freire, C., De Lima Neto, P., Correia, A.N., Oliveira, M.B.P.P., Delerue Matos, C., 2013. Biosens. Bioelectron. 47, 292–299.

Pardo Yissar, V., Katz, E., Wasserman, J.L., Willner, I., 2003. J. Am. Chem. Soc. 125, 622–623.

Periasamy, A.P., Umasankar, Y., Chen, S.M., 2009. Sensors 9, 4034–4055.

Qian, S.H., Lin, H.W., 2015. Anal. Chem. 87(10), 5395–5400.

Rao, T.N., Sarada, B.V., Terashima, C., Fujishima, A., 2002. Anal. Chem. 74(7), 1578–1583.

Schulze, H., Vorlová, S., Villatte, F., Bachmann, T.T., Schmid, R.D., 2003. Biosens. Bioelectron. 18(2–3), 201–209.

Seiber, J.N., Kleinschmidt, L.A., 2011. J. Agric. Food Chem. 59(14), 7536–7543.

Shi, L., Chu, Z.Y., Liu, Y., Jin, W.Q., Chen, X.J., 2014. Biosens. Bioelectron. 54, 165–170.

Song, Y., Li, W.K., Duan, Y.F., Li, Z.J., Deng, L., 2014. Biosens. Bioelectron. 55, 400–404.

Suwansa ard, S., Kanatharana, P., Asawatreratanakul, P., Limsakul, C., Wongkittisuksa, B., Thavarungkul, P., 2005. Biosens. Bioelectron. 21(3), 445–454.

Tang, L.H., Liu, Y., Ali, M.M., Kang, D.K., Zhao, W.A., Li, J.H., 2012. Anal. Chem. 84(11), 4711–4717.

Upadhyay, S., Rao, G.R., Sharma, M.K., Bhattacharya, B.K., Rao, V.K., Vijayaraghavan, R., 2009. Biosens. Bioelectron. 25(4), 832–838.

Wang, J., Cheung, W., Leung, D., 2014a. J. Agric. Food Chem. 62(4), 966–983.

Wang, X.Z., Hou, T., Lu, T.T., Li, F., 2014b. Anal. Chem. 86(19), 9626–9631.

Xing, X.J., Zhou, Y., Liu, X.G., Pang, D.W., Tang, H.W., 2014. Small 10(16), 3412–3420.

Yao, G.H., Liang, R.P., Huang, C.F., Wang, Y., Qiu, J.D., 2013. Anal. Chem. 85, 11944–11951.

Yi, Y.H., Zhu, G.B., Liu, C., Huang, Y., Zhang, Y.Y., Li, H.T., Zhao, J.N., Yao, S.Z., 2013. Anal. Chem. 85, 11464–11470.

Yuan, M., Zhu, Y.G., Lou, X.H., Chen, C., Wei, G., Lan, M.B., Zhao, J.L., 2012. Anal. Methods 4, 2846–2851.

Zamfir, L.G., Rotariu, L., Bala, C., 2013. Biosens. Bioelectron. 46, 61–67.

Zhang, G.F., Zhan, J.Y., Li, H.B., 2011. Org. Lett. 13(13), 3392–3395.

Zhang, M.W., Cao, X.Y., Li, H.K., Guan, F.R., Guo, J.J., Shen, F., Luo, Y.L., Sun, C.Y., Zhang, L.G., 2013a. Anal. Methods 5, 6830–6838.

Zhang, Y., Cai, Y., Qi, Z., Lu, L., Qian, Y., 2013b. Anal. Chem. 85, 8455–8461.

Zhao, W.W., Shan, S., Ma, Z.Y., Wan, L.N., Xu, J.J., Chen, H.Y., 2013. Anal. Chem. 85, 11686–11690.

Zhou, T., Xiao, X.H., Li, G.K., 2012. Anal. Chem. 84(13), 5816–5822.

Zhou, Z.M., Chen, J.B., Zhao, D.Y., Yang, M.M., 2009. J. Agric. Food Chem. 57, 8722–8727.

Zhu, G.C., Li, Y., Zhang, C.Y., 2014. Chem. Commun. 50, 572–574.

Table 1 Sequences of the oligonucleotides used in this work[a]

Figure Captions

Fig. 1. Schematic illustration of the fluorescence assay for aldicarb based on Hg^{2+}-mediated DNA probe and nicking enzyme assisted cycling amplification reaction.

Fig. 2. Fluorescence spectra of the assay system under different conditions: (a) QFP; (b) QFP + HP1; (c) QFP + HP1 + Nb.BtsI enzyme; (d) QFP + HP1 +ACh + Nb.BtsI enzyme; (e) QFP + HP + ACh + AChE + Nb.BtsI enzyme; (f) QFP + HP1 + ACh + AChE + Aldicarb + Nb.BtsI enzyme. The concentrations of QFP, HP1, ACh, AChE, Aldicarb and Nb.BtsI enzyme were 250 nM, 5 nM, 0.03 μM, 1 mU mL^{-1}, 200 μg L^{-1} and 100 U mL^{-1}, respectively.

Fig. 3. The effect of AChE concentration (A) and pH (B) on fluorescence intensity. The error bars represent the standard deviation of three measurements. The concentrations of QFP, HP1, ACh, AChE and Nb.BtsI enzyme were 250 nM, 5 nM, 0.03 μM, 1 mU mL^{-1} and 100 U mL^{-1}, respectively.

Fig. 4. The effect of temperature (A) and hydrolysis reaction time of ACh (B) on the fluorescence intensity. The error bars represent the standard deviation of three measurements. For other conditions, see Fig. 3.

Fig. 5. (A) Fluorescence emission spectra of the biosensing platform in the presence of aldicarb with different concentrations: (a) 0, (b) 10, (c) 100, (d) 200, (e) 500, (f) 1000, (g) 2000, (h) 4000, (i) 6000, (j) 8000, (k) 10000 μg L^{-1}. (B) Calibration curve corresponding to the fluorescence intensity as a function of aldicarb concentration. Inset shows the linear relationship between the fluorescence intensity and the logarithm of the aldicarb concentration. The error bars represent the standard deviation of three measurements. For other conditions, see Fig. 3.

a

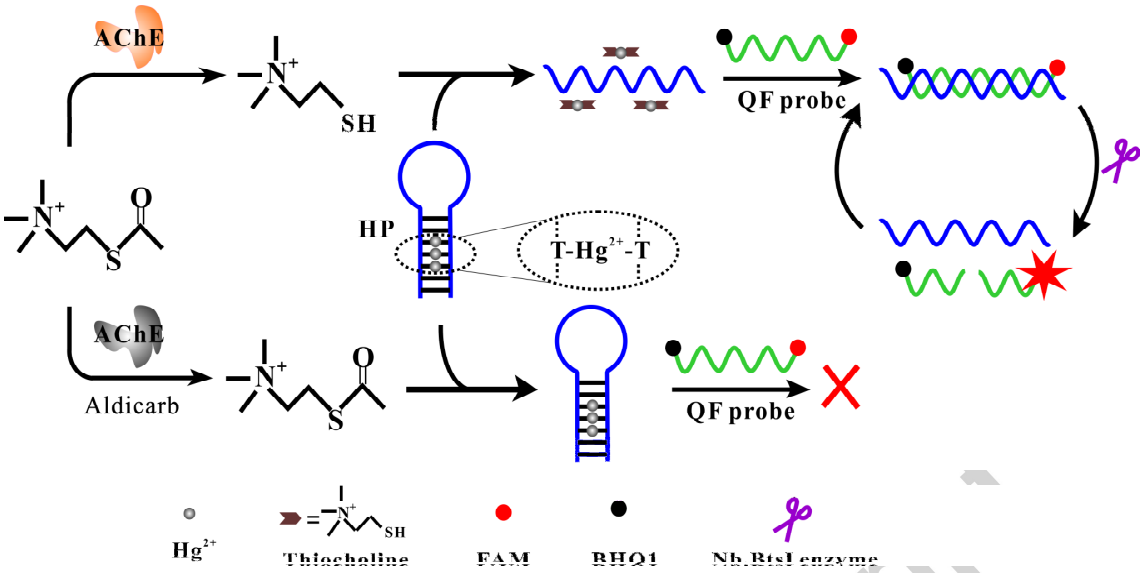

Fig. 1

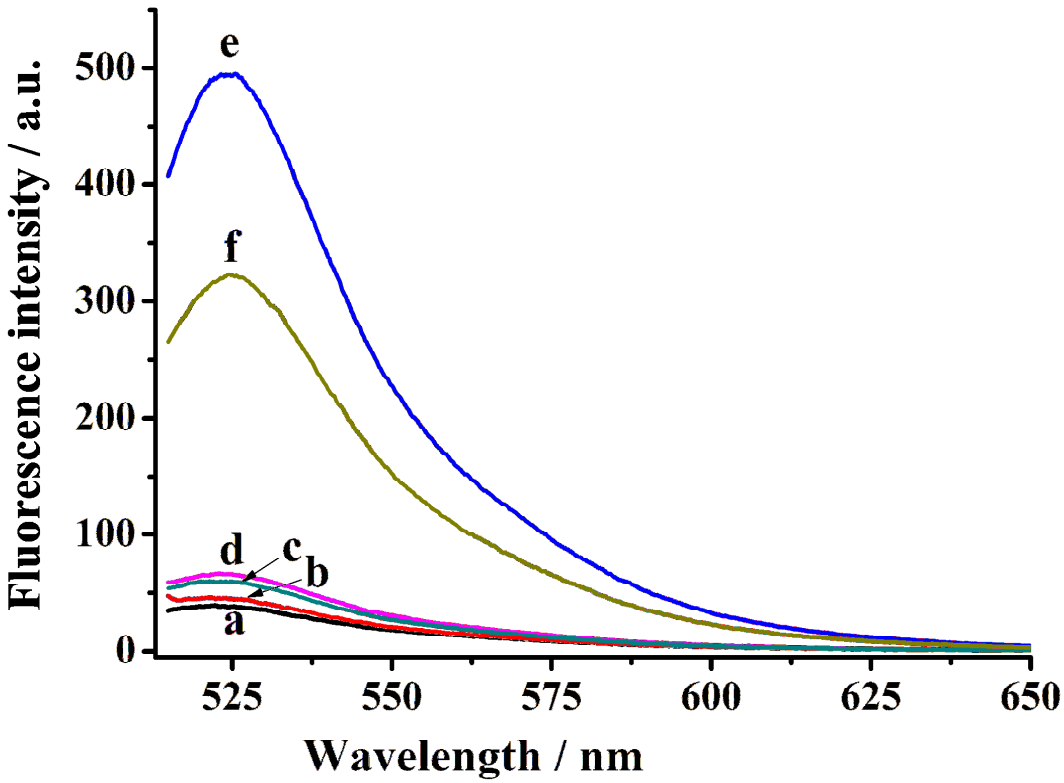

Fig. 2

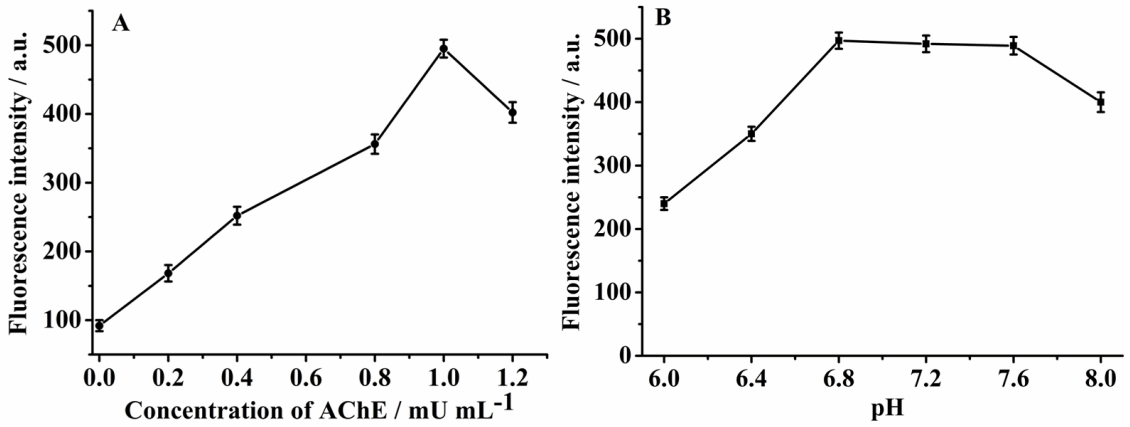

Fig. 3

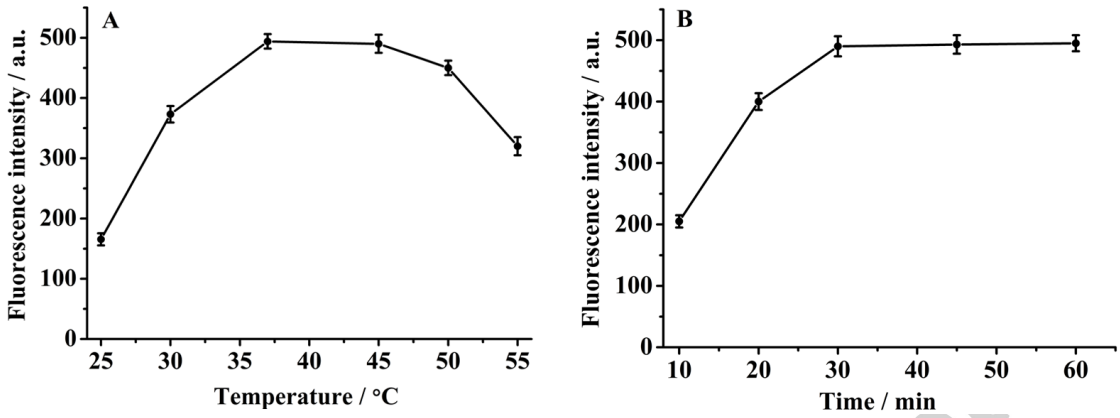

Fig. 4

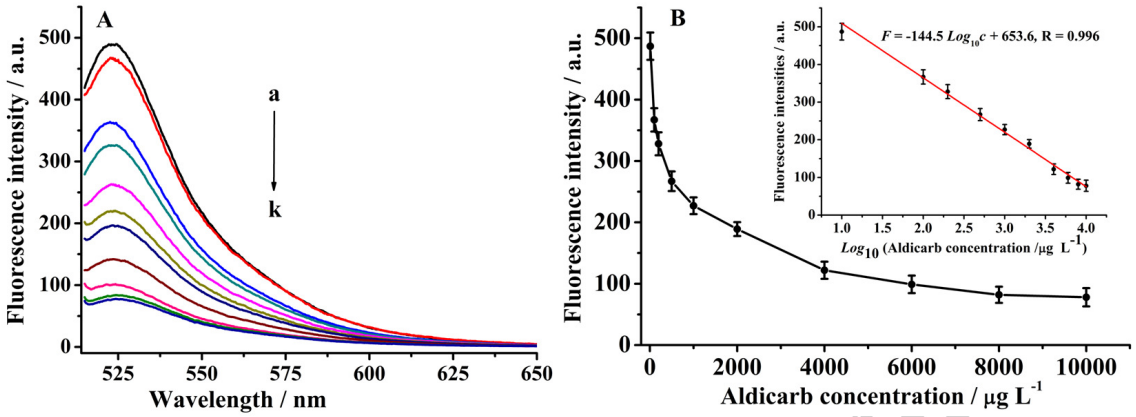

Fig. 5

Highlights

> A highly sensitive fluorescent biosensor for the detection of carbamate pesticides has been proposed. >It is based on acetylcholinesterase-catalyzed hydrolysis triggered Hg^{2+}-mediated DNA conformational switch and nicking enzyme-assisted cycling amplification. > The detection limit of the model analyte aldicarb is 3.3 μg L^{-1}, which is much lower than the Chinese National Standards or those previously reported in literature.

Table 1 Sequences of the oligonucleotides used in this work[a]

Name	Sequence (5′ – 3′)
Helper probe 1 (HP1)	CGTTTCA *GCAGTG* TTTCG
Helper probe 2 (HP2)	AGCAGTGTT
QF probe (QFP)	FAM– AA_{Δ}*CACTGC*T–BHQ1

[a] The letters in italic represent the Nb.BtsI recognition sequences, the underlined letters represent the sequences that form a duplex through T- Hg^{2+}-T mismatch in the presence of Hg^{2+}. FAM and BHQ1 represent 5-carboxyfluoescein, and black hole quencher, respectively. "Δ" represents Nb.BtsI enzyme cleavage site.